Proteasome Inhibition

International Edition: DOI: 10.1002/anie.201505054
German Edition: DOI: 10.1002/ange.201505054

Identification of a β1/β2-Specific Sulfonamide Proteasome Ligand by Crystallographic Screening

*Philipp Beck, Michèle Reboud-Ravaux, and Michael Groll**

Abstract: *The proteasome represents a validated drug target for the treatment of cancer, however, new types of inhibitors are required to tackle the development of resistant tumors. Current fluorescence-based screening methods suffer from low sensitivity and are limited to the detection of ligands with conventional binding profiles. In response to these drawbacks, a crystallographic screening procedure for the discovery of agents with a novel mode of action was utilized. The optimized workflow was applied to the screening of a focused set of compounds, resulting in the discovery of a β1/β2-specific sulfonamide derivative that noncovalently binds between subunits β1 and β2. The binding pocket displays significant differences in size and polarity between the immuno- and constitutive proteasome. The identified ligand thus provides valuable insights for the future structure-based design of subtype-specific proteasome inhibitors.*

The fight against oncological diseases requires a permanent search for chemical agents that block cellular pathways that are indispensable for the survival of cancer cells. The 20S proteasome (core particle; CP) was identified as such a target owing to its central role in protein quality control, protein turnover, cell-cycle regulation, cell differentiation, and apoptosis. Indeed, FDA approval of the CP inhibitors bortezomib (BTZ, Velcade) and carfilzomib (CFZ, Kyprolis) confirmed that blocking proteasomal activity is beneficial for the treatment of multiple myeloma and mantle cell lymphoma (Figure S1 in the Supporting Information).[1,2] The two agents share a similar peptidic scaffold with an electrophilic warhead for covalent binding to the catalytic Thr1 residues of the protease, and the development of resistance against both agents highlights the need for non-peptidic inhibitors.[3–8] In addition, the development of the next generation of proteasome blockers has to focus on selectively addressing the constitutive CP (cCP) and tissue-specific proteasomal subtypes that play crucial roles in autoimmune or inflammatory diseases (immunoproteasome, iCP) as well as T cell development in the thymus (thymoproteasome, tCP).[9–11]

[*] Dr. P. Beck, Prof. Dr. M. Groll
Center for Integrated Protein Science Munich (CIPSM)
Department of Chemistry, Technische Universität München
Lichtenbergstraße 4, 85748 Garching (Germany)
E-mail: michael.groll@tum.de
Prof. Dr. M. Reboud-Ravaux
Sorbonne Universités, UPMC Univ Paris 06, UMR/CNRS 8256
Case 256, 7 Quai St-Bernard, 75252 Paris Cedex 05 (France)

Supporting information for this article is available on the WWW under http://dx.doi.org/10.1002/anie.201505054.

Recently, the discovery of *N*-hydroxyureas and alkaloids as proteasome inhibitors broadened the range of potential scaffolds.[12,13] In addition to the scientific literature, some innovative scaffolds have been revealed in patents,[14–18] but apart from these advances, the general structure of validated CP inhibitors has historically been limited to peptidic pharmacophores.[19,20] Concurrently, the development of new proteasome blockers continues to be hampered by a lack of structural knowledge from ligands that target novel binding sites since common fluorescence-based screening methods suffer from two major limitations. First, the assays are susceptible to fluorescence quenching artifacts, thus resulting in a high number of false-positive or false-negative results. Second, the employed chromogenic substrates are unsuitable for the detection of weakly binding fragments or ligands that populate allosteric sites. In addition, screening with biophysical methods like isothermal calorimetry, surface plasmon resonance, or NMR are hampered by the large size and demanding architecture of the CP.

To address these drawbacks, we applied a crystallographic screening procedure for the rapid evaluation of focused compound libraries (Scheme 1). The purification and crystallization of yeast CPs (yCP) is well documented and results in an abundance of high-quality crystals for compound soaking.[21] By using recent advances in synchrotron automation and dataset evaluation software, we established an accelerated workflow that includes crystal mounting, dataset collection, data reduction, refinement, and subsequent automated ligand search in less than 10 min per dataset (Scheme 1).[22]

For the evaluation of our crystallographic screening approach, we assembled a focused set of compounds that were expected to show novel binding modes and furthermore fulfilled the following criteria (Scheme S2 and Table S1 in the Supporting Information):

a) Representation of a vast variety of chemotypes with predominantly non-peptidic scaffolds.
b) Compounds that have previously been reported to act as CP inhibitors in vitro or in cell culture studies.
c) Lack of structural data for the respective ligands bound to the CP.
d) Simple chemical synthesis, commercial availability, or availability through collaborators (Figure S2 in the Supporting Information).

Following our setup, yeast 20S proteasome crystals were soaked with the screening compounds and diffraction data were recorded to a maximum resolution of about 2.6 Å within 3 min. Rigid-body refinement using yCP as starting coordinates (PDB ID 1RYP)[21] yielded R_{free} values below 25% within another 3 min. Subsequent automated searching of the

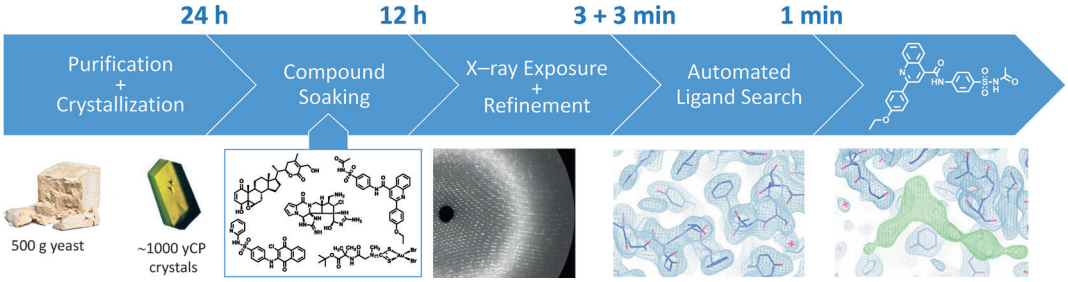

Scheme 1. Workflow of the optimized crystallographic screening approach for identifying novel proteasome ligands.

resulting F_o-F_c map visualized the presence of any ligand-related positive electron density (< 1 min). Our method was verified with the identification of the non-peptidic sulfonamide **1** as a hit, a compound that has been reported as a putative CP inhibitor in an in silico screening study for novel β5 inhibitors.[23] However, the ligand turned out to selectively block the β1 and β2 activities, while β5 remained unaffected. This unusual inhibition profile led to its incorporation into the compound set and the application of **1** in our screening workflow to give a yCP:**1** cocrystal structure (R_{free} = 21.4%, PDB ID 5BOU).

Surprisingly, inspection of the crystallographic data revealed that the non-primed substrate binding channels of all of the catalytic sites lacked any ligand-related electron density. Instead, **1** was located at the primed site of subunit β2, which represents a hitherto unobserved binding pocket in the proteasome (Figure 1). The ligand bridges the entire length of the primed β2 substrate binding channel, forming extensive hydrophilic and hydrophobic interactions. In particular, the sulfonyl oxygen atoms of **1** are tightly coordinated by β2-Thr1O$^{\gamma}$H, β2-Thr1NH$_3^+$, and β2-Gly47NH, thus disrupting key residues that stabilize the tetrahedral transition state of substrates during catalytic peptide-bond cleavage (Figure 1). In addition, the 2,4-substituted quinoline ring system protrudes deeply into a large cavity that is formed by residues of both the β2 and β1 subunits. The binding of **1** is thereby favored by van-der-Waals interactions with L127, Y97, and H114 (all β2), as well as β1-Y25, while a single polar interaction between β1-T22O$^{\gamma}$H and the quinoline nitrogen atom provides additional stabilization.

Interestingly, structural superposition of yCP:**1** and yCP in complex with the tetrapeptidic inhibitor carfilzomib revealed that the 4′-ethoxyphenyl moiety of **1** is in close contact with β2-H116, which participates in the formation of the S4 substrate specificity pocket of subunit β1 (Figure 1 and Figure 2).[24] These findings explain why **1** is able to inhibit both the β1 and β2 catalytic sites (inhibitor concentration giving 50% inhibition (IC_{50}) ≈ 100 and 50 μM, respectively), while the chymotrypsin-like activity remains unaffected.[23] First, the sulfonyl moiety of the ligand forms hydrogen bonds with β2-Thr1 and thus impairs peptide bond hydrolysis at the β2 subunit. Second, the biaryl system of **1** stretches into the substrate binding channel of the β1 subunit, thereby affecting substrate turnover. Notably, the reported high micromolar IC_{50} values for **1** are only a rough indication of the binding strength since the applied peptidic substrates do not compete against ligand binding in the primed site. As a result,

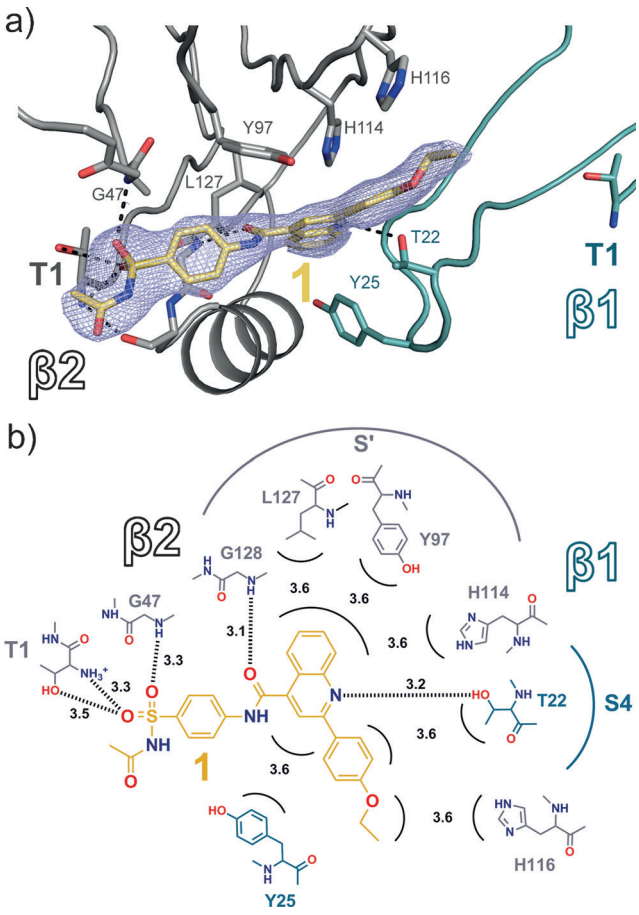

Figure 1. Crystal structure of yCP in complex with **1**. a) 2 F_O-F_C electron density map (blue mesh, 1σ, PDB ID 5BOU) of **1** (yellow) located at the primed site of the β2 substrate binding channel (gray). The sulfonyl group of **1** forms a network of hydrogen bonds (black dashed lines) with β2-Thr1O$^{\gamma}$H, β2-Thr1NH$_3^+$, and β2-Gly47NH, thereby disrupting the hydrogen-bonding network at Thr1 and the oxyanion hole, respectively. b) Schematic overview of (a). The interaction distances are shown in Å. The amino acids of β1 and β2 are colored in teal and gray, respectively.

structure–activity-guided ligand optimization is limited by the shortcomings of current in vitro CP activity assays that make use of non-natural substrate mimetics.

Next, we aimed to employ a crystallographic approach to determine the minimal requirements for ligand binding in the newly discovered site. The sulfonamide compound **1** consists of a restrained, conjugated scaffold with a limited number of

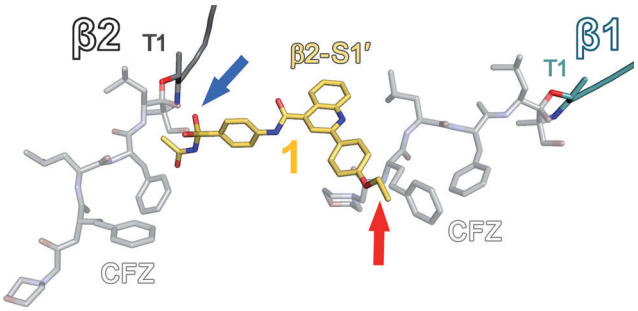

Figure 2. Bivalent targeting of subunits β1 and β2. Structural superposition of **1** (yellow) and CFZ (gray)[24] bound to the β1 and β2 active sites of yCP illustrates the combined effect of the ligand to competitively and noncovalently block both catalytic activities. The sulfonyl group of **1** is in close contact with Thr1 (blue arrow), while its 4′-ethoxyphenyl moiety protrudes into the S4 specificity pocket of subunit β1 (red arrow).

rotatable bonds, which minimizes the entropic penalty that has to be overcome during the binding process. As a result, most of the contributions to yCP:**1** complex formation must originate from favorable enthalpic gains from the interactions depicted in Figure 1 b. Indeed, for the known sulfonamide antibiotic sulfacetamide **2** as well as the synthesized ligand fragments **3** and **4** (Figure S3 in the Supporting Information), no defined electron density for the compounds could be obtained in the recorded datasets. Therefore, only the combination of the biaryl quinoline and the sulfacetamide motif gives a sufficient gain in enthalpic energy for complex formation, thus representing an important precondition for a fragment evolution approach.

In spite of recent advances, the development of iCP-specific ligands is hampered by the limited structural diversity of inhibitor binding sites among the proteasomal subtypes.[25,26] However, comparison of the primed substrate binding channels of β2c and β2i highlights extraordinary structural differences between these two isoforms.[11,27] This is illustrated by superposition of the binding site of **1** with the murine β2c and β2i subunits, which reveals that the respective β2-S′ pockets display significant differences in size and polarity (Scheme 2). Specifically, amino acid replacements in the iCP, including β2-S131Q and β1-A27V, result in a smaller and more polar S′ pocket. This knowledge will enable future efforts toward the structure-based design of specific ligands.

In summary, the introduced crystallographic screening method identified a sulfonamide derivative as a novel proteasome ligand. Its unique binding properties provide potential for further optimization in the following ways (Scheme 2):

a) The sulfonyl group forms a tight hydrogen-bonding network with residues involved in catalysis at subunit β2.
b) Ligand growing is possible towards the β1 substrate binding channel through extension of the 4′-ethoxyphenyl group that already protrudes into the S4 pocket of subunit β1.
c) Variation of the quinoline ring motif (blue) enables selectivity regarding either β2c or β2i.

Taken together, the herein presented crystallographic screening procedure resulted in the identification of sulfonamide **1** as a promising noncovalent proteasome ligand. The newly discovered binding site is located between the β2-S′ primed and β1 non-primed substrate binding channel and displays significant differences in size and polarity between iCP and cCP. The highly constrained ligand results in a predominantly enthalpy-controlled binding event, which in general is a driving force for target selectivity.[28] Moreover, the absence of the pharmacokinetically unfavorable reactive headgroups and peptidic scaffold of traditional CP inhibitors qualifies the ligand for further optimization towards a highly active non-peptidic proteasome inhibitor.

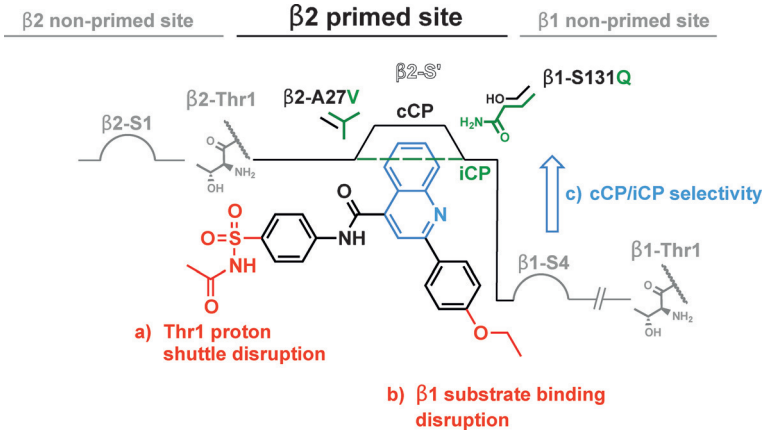

Scheme 2. Schematic representation of the essential structural characteristics of **1** that contribute to its selective binding affinity. The β2-S′ pocket of cCP and iCP are represented as a solid black or dashed green line, respectively.

Acknowledgements

This work was funded by the DFG GR 1861/10-1. We are grateful to our collaborators who helped us to assemble the screening set. We thank the staff of the beamline X06SA at the Paul Scherrer Institute, Swiss Light Source, Villigen (Switzerland) for assistance during data collection and R. Feicht for large-scale purification and crystallization of yeast 20S proteasomes.

Keywords: crystallographic screening · drug discovery · proteasome · reversible inhibition · sulfonamides

How to cite: *Angew. Chem. Int. Ed.* **2015**, *54*, 11275–11278
Angew. Chem. **2015**, *127*, 11428–11431

[1] P. G. Richardson, T. Hideshima, K. C. Anderson, *Cancer Control* **2003**, *10*, 361–369.
[2] S. D. Demo, C. J. Kirk, M. A. Aujay, T. J. Buchholz, M. Dajee, M. N. Ho, J. Jiang, G. J. Laidig, E. R. Lewis, F. Parlati et al., *Cancer Res.* **2007**, *67*, 6383–6391.

[3] M. Groll, C. R. Berkers, H. L. Ploegh, H. Ovaa, *Structure* **2006**, *14*, 451 – 456.
[4] M. Groll, K. B. Kim, N. Kairies, R. Huber, C. M. Crews, *J. Am. Chem. Soc.* **2000**, *122*, 1237 – 1238.
[5] R. Z. Orlowski, D. J. Kuhn, *Clin. Cancer Res.* **2008**, *14*, 1649 – 1657.
[6] V. Cheriyath, B. S. Jacobs, M. A. Hussein, *Drugs R&D* **2007**, *8*, 1 – 12.
[7] D. J. McConkey, K. Zhu, *Drug Resist. Updates* **2008**, *11*, 164 – 179.
[8] W. Harshbarger, C. Miller, C. Diedrich, J. Sacchettini, *Structure* **2015**, *23*, 418 – 424.
[9] M. Groettrup, R. Kraft, S. Kostka, S. Standera, R. Stohwasser, P.-M. Kloetzel, *Eur. J. Immunol.* **1996**, *26*, 863 – 869.
[10] S. Murata, K. Sasaki, T. Kishimoto, S.-I. Niwa, H. Hayashi, Y. Takahama, K. Tanaka, *Science* **2007**, *316*, 1349 – 1353.
[11] E. M. Huber, M. Basler, R. Schwab, W. Heinemeyer, C. J. Kirk, M. Groettrup, M. Groll, *Cell* **2012**, *148*, 727 – 738.
[12] N. Gallastegui, P. Beck, M. Arciniega, R. Huber, S. Hillebrand, M. Groll, *Angew. Chem. Int. Ed.* **2012**, *51*, 247 – 249; *Angew. Chem.* **2012**, *124*, 251 – 254.
[13] P. Beck, T. A. Lansdell, N. M. Hewlett, J. J. Tepe, M. Groll, *Angew. Chem. Int. Ed.* **2015**, *54*, 2830 – 2833; *Angew. Chem.* **2015**, *127*, 2872 – 2875.
[14] S. M. Lynch, W. Neidhart, J. M. Plancher, T. Schulz-Gasch, WO 2014086664, **2014**.
[15] "Substituted Thiazole Compounds": R. C. Hawley, S. M. Lynch, WO 2014114603A1, **2014**.
[16] "Substituted Thiazole Compounds": M. Alam, R. C. Hawley, S. M. Lynch, A. Narayanan, WO 2014086701A1, **2014**.
[17] "Substituted Thiazole Compounds": Stephen M. Lynch, A. Narayanan, WO 2014086697A1, **2014**.
[18] "Substituted Triazole And Imidazole Compounds": S. M. Lynch, R. E. Martin, W. Neidhart, J.-M. Plancher, T. Schulz-Gasch, WO2014/086663A1, **2014**.
[19] A. F. Kisselev, W. a van der Linden, H. S. Overkleeft, *Chem. Biol.* **2012**, *19*, 99 – 115.
[20] C. Blackburn, C. Barrett, J. L. Blank, F. J. Bruzzese, N. Bump, L. R. Dick, P. Fleming, K. Garcia, P. Hales, M. Jones et al., *MedChemComm* **2012**, *3*, 710.
[21] M. Groll, L. Ditzel, J. Lowe, D. Stock, M. Bochtler, H. D. Bartunik, R. Huber, *Nature* **1997**, *386*, 463 – 471.
[22] M. Groll, R. Huber, *Methods Enzymol.* **2005**, *398*, 329 – 336.
[23] N. Basse, M. Montes, X. Maréchal, L. Qin, M. Bouvier-Durand, E. Genin, J. Vidal, B. O. Villoutreix, M. Reboud-Ravaux, *J. Med. Chem.* **2010**, *53*, 509 – 513.
[24] E. M. Huber, W. Heinemeyer, M. Groll, *Structure* **2015**, *23*, 407 – 417.
[25] C. Dubiella, H. Cui, M. Gersch, A. J. Brouwer, S. A. Sieber, A. Krüger, R. M. J. Liskamp, M. Groll, *Angew. Chem. Int. Ed.* **2014**, *53*, 11969 – 11973; *Angew. Chem.* **2014**, *126*, 12163 – 12167.
[26] G. de Bruin, E. M. Huber, B. Xin, E. J. van Rooden, K. Al-Ayed, K. Kim, A. F. Kisselev, C. Driessen, M. van der Stelt, G. A. van der Marel et al., *J. Med. Chem.* **2014**, *57*, 6197 – 6209.
[27] E. M. Huber, M. Groll, *Angew. Chem. Int. Ed.* **2012**, *51*, 8708 – 8720; *Angew. Chem.* **2012**, *124*, 8838 – 8850.
[28] H. Gohlke, G. Klebe, *Angew. Chem. Int. Ed.* **2002**, *41*, 2644 – 2676; *Angew. Chem.* **2002**, *114*, 2764 – 2798.

Received: June 3, 2015
Revised: July 3, 2015
Published online: August 4, 2015

